


## ARTICLE

# Optimizing the biosynthesis of oxygenated and acetylated Taxol precursors in *Saccharomyces cerevisiae* using advanced bioprocessing strategies

Laura E. Walls<sup>1,2,3</sup>  | Koray Malcı<sup>1,2</sup> | Behnaz Nowrouzi<sup>1,2</sup> | Rachel A. Li<sup>4,5</sup> | Leo d'Espaux<sup>4,5</sup> | Jeff Wong<sup>4,5</sup> | Jonathan A. Dennis<sup>2,6</sup> | Andrea J. C. Semião<sup>7</sup> | Stephen Wallace<sup>2,6</sup> | José L. Martinez<sup>3</sup> | Jay D. Keasling<sup>4,5,8,9,10</sup> | Leonardo Rios-Solis<sup>1,2</sup>

<sup>1</sup>Institute for Bioengineering, School of Engineering, University of Edinburgh, Edinburgh, UK

<sup>2</sup>Centre for Synthetic and Systems Biology (SynthSys), University of Edinburgh, Edinburgh, UK

<sup>3</sup>Department of Biotechnology and Biomedicine, Section for Synthetic Biology, Technical University of Denmark, Kongens Lyngby, Denmark

<sup>4</sup>DOE Joint BioEnergy Institute, Emeryville, California, USA

<sup>5</sup>Division of Biological Systems and Engineering, Lawrence Berkeley National Laboratory, Berkeley, California, USA

<sup>6</sup>Institute of Quantitative Biology, Biochemistry, and Biotechnology, School of Biological Sciences, University of Edinburgh, Edinburgh, UK

<sup>7</sup>Institute for Infrastructure and Environment, School of Engineering, University of Edinburgh, Edinburgh, UK

<sup>8</sup>Center for Biosustainability, Danish Technical University, Lyngby, Denmark

<sup>9</sup>Center for Synthetic Biochemistry, Institute for Synthetic Biology, Shenzhen Institutes for Advanced Technologies, Shenzhen, China

<sup>10</sup>Departments of Chemical and Biomolecular Engineering and of Bioengineering, University of California, Berkeley, Berkeley, California, USA

## Correspondence

Leonardo Rios-Solis, Institute for Bioengineering, School of Engineering, University of Edinburgh, Kings Buildings, Edinburgh, UK.

Email: [Leo.Rios@ed.ac.uk](mailto:Leo.Rios@ed.ac.uk)

## Funding information

Engineering and Physical Sciences Research Council, Grant/Award Number: EP/R513209/1; Ministry of National Education of the Republic of Turkey; University of Edinburgh: The University of Edinburgh Principal's Career Development PhD Scholarship; Royal Society, Grant/Award Number: RSG\R1\180345; University of Edinburgh Global Challenges Theme Development Fund 418, Grant/Award Number: TDF\_03; US National Science Foundation, Grant/Award Number: 1330914; Novo Nordisk Foundation, Grant/Award Number: NNF17SA0031362

## Abstract

Taxadien-5 $\alpha$ -hydroxylase and taxadien-5 $\alpha$ -ol O-acetyltransferase catalyze the oxidation of taxadiene to taxadien-5 $\alpha$ -ol and subsequent acetylation to taxadien-5 $\alpha$ -yl-acetate in the biosynthesis of the blockbuster anticancer drug, paclitaxel (Taxol®). Despite decades of research, the promiscuous and multispecific CYP725A4 enzyme remains a major bottleneck in microbial biosynthetic pathway development. In this study, an interdisciplinary approach was applied for the construction and optimization of the early pathway in *Saccharomyces cerevisiae*, across a range of bioreactor scales. High-throughput microscale optimization enhanced total oxygenated taxane titer to 39.0  $\pm$  5.7 mg/L and total taxane product titers were comparable at micro and minibioreactor scale at 95.4  $\pm$  18.0 and 98.9 mg/L, respectively. The introduction of pH control successfully mitigated a reduction of oxygenated taxane production, enhancing the potential taxadien-5 $\alpha$ -ol isomer titer to 19.2 mg/L, comparable with the 23.8  $\pm$  3.7 mg/L achieved at microscale. A combination of bioprocess optimization and increased gas chromatography-mass spectrometry resolution at 1 L bioreactor scale facilitated taxadien-5 $\alpha$ -yl-acetate detection with a final titer of 3.7 mg/L.

Koray Malcı, Behnaz Nowrouzi, and Rachel A. Li contributed equally as second authors.

This is an open access article under the terms of the Creative Commons Attribution License, which permits use, distribution and reproduction in any medium, provided the original work is properly cited.

© 2020 The Authors. *Biotechnology and Bioengineering* published by Wiley Periodicals LLC

Total oxygenated taxane titers were improved 2.7-fold at this scale to 78 mg/L, the highest reported titer in yeast. Critical parameters affecting the productivity of the engineered strain were identified across a range of scales, providing a foundation for the development of robust integrated bioprocess control systems.

#### KEYWORDS

high throughput microbioreactor, *Saccharomyces cerevisiae*, taxadien-5- $\alpha$ -ol O-acetyltransferase, taxadien-5-hydroxylase, Taxol

## 1 | INTRODUCTION

Paclitaxel (Taxol<sup>®</sup>) is one of the most widely administered chemotherapeutic agents owing to its effectiveness against a vast range of diseases. Although it is found naturally in the bark of Pacific Yew (*Taxus brevifolia*), the destruction of three mature trees is necessary to yield just 1 g of paclitaxel (McElroy & Jennewein, 2018), rendering direct extraction unsustainable. Heterologous expression of the complex biosynthetic pathway using a fast-growing eukaryotic host could provide a sustainable solution. However, the pathway is yet to be fully elucidated and low and variable titers of the early precursors have been achieved to date (Liu et al., 2016; McElroy & Jennewein, 2018).

The first committed step in paclitaxel biosynthesis involves the cyclization of geranylgeranyl diphosphate (GGPP), a product of the mevalonate pathway, by taxadiene synthase (TASY), yielding taxa-4(5),11(12)-diene (taxadiene) and its structural isomer taxa-4(20),11(12)-diene (iso-taxadiene) as shown in Figure 1.

Both compounds are substrates for the subsequent enzyme taxadien-5 $\alpha$ -hydroxylase (CYP725A4), which is the first of several cytochrome P450s in the paclitaxel pathway (Jennewein et al., 2004). The desired product of this first oxidation reaction is taxadien-5 $\alpha$ -ol (T5 $\alpha$ ol), which subsequently undergoes acetylation in the third step in the pathway in a reaction catalyzed by taxadien-5- $\alpha$ -ol O-acetyltransferase (TAT), yielding taxa-4(20),11-dien-5 $\alpha$ -yl acetate (Walker et al., 1999).

Heterologous expression of TASY and CYP725A4 has been accomplished using both *Saccharomyces cerevisiae* (DeJong et al., 2006; Edgar et al., 2016) and *Escherichia coli* (Edgar et al., 2016; Sagwan-Barkdoll & Anterola, 2018; Yadav, 2014). Although, taxadiene titers of up to 1 g/L have been achieved in *E. coli*, when CYP725A4 was subsequently expressed in the respective strain, a significant drop in productivity was observed, with a total oxygenated taxane titer of 116 mg/L (Ajikumar et al., 2010). An impressive effort was made to optimize P450 expression and reductase partner interactions in *E. coli*, achieving a fivefold improvement in total oxygenated taxanes to 570 mg/L (Biggs et al., 2016). However, the overexpression of the subsequent cytochrome P450s in the paclitaxel pathway is likely to be very challenging in the prokaryotic host. On the other hand, the eukaryotic host, *S. cerevisiae*, possesses the necessary biosynthetic and redox capabilities for the expression of such enzymes (Engels et al., 2008). Despite this, the maximum reported taxadiene titers are

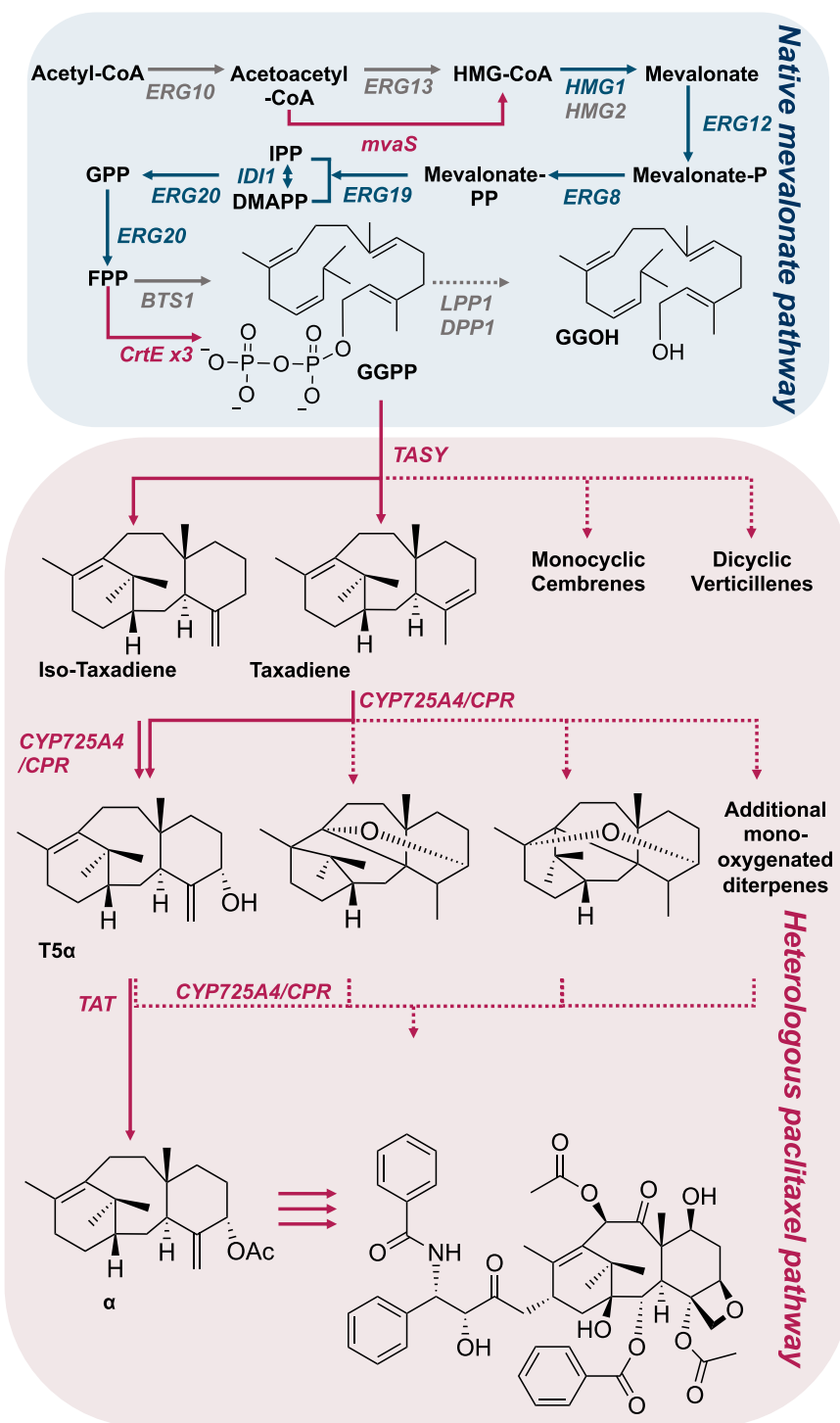
eightfold lower in yeast (Nowrouzi et al., 2020). Distributing the early Taxol metabolic pathway among *E. coli* and *S. cerevisiae* facilitated a total oxygenated taxane titer of 33 mg/L (Zhou et al., 2015).

Microbial expression of CYP725A4 has resulted in a wide range of side products including OCT and iso-OCT (Figure 1) and the desired T5 $\alpha$ ol compound was a minor product when expressed in *E. coli* (Sagwan-Barkdoll & Anterola, 2018). Additional studies reported further unknown monooxygenated and dioxygenated taxane compounds (Edgar et al., 2016; Yadav, 2014). In addition to variations in the nature of the oxygenated taxanes produced, the ratios of the products generated differed substantially. Edgar et al. (2016) reported that T5 $\alpha$ ol comprised between 0% and 25% of the products of CYP725A4 depending on the microbial host, growth medium, and extraction procedure used. Variations in process conditions between these steps may contribute to the observed product distributions. Despite extensive improvements in the microbial expression of the first two enzymes in the paclitaxel biosynthetic pathway, progress toward the construction of the third step has been limited. Early characterization studies revealed TAT is also multispecific (Walker et al., 1999). Several isoprenoid alcohols including GGOH and farnesol were found to be substrates of the enzyme. Despite this, when TAT was heterologously expressed along with TASY and CYP725A4 in *E. coli*, of the several mono and dioxygenated CYP725A4 products, only T5 $\alpha$ ol appeared to undergo acetylation (Edgar et al., 2016).

Traditionally, simple small scale shake flask or microplate cultures have been exploited for early-stage bioprocess development (Doran, 1995; Funke et al., 2010). However, such systems offer limited insight to the nature of the process and there are major discrepancies in cultivation strategies across scales (Funke et al., 2010). As a result, their use has often resulted in the selection of suboptimal production conditions, leading to setbacks at the manufacturing stage (Yu et al., 2014). Maximizing process understanding during the earliest stages of bioprocess development is essential to overcome such issues. To tackle this, scalable high-throughput screening systems have been developed, allowing industrial bioreactor conditions to be more closely mimicked (Back et al., 2016; Funke et al., 2009; Kensy et al., 2009; Kostov et al., 2001). Through coupling such instruments with a strategic design of experiments approach, factors can be manipulated to statistically determine relationships between parameters and performance, ensuring quality by design.

This study aimed to develop a robust bioprocess for paclitaxel precursor production using *S. cerevisiae* microbial cell

**FIGURE 1** Engineered biosynthetic pathway in *Saccharomyces cerevisiae*. (a) The pathway highlighted in blue is the native mevalonate pathway; a product of this is the universal diterpenoid precursor, GGPP. The first enzyme in the paclitaxel pathway (highlighted in red), TASY catalyzes the conversion of GGPP yielding taxadiene and small amounts of its isomer iso-taxadiene. The second enzyme CYP725A4, coupled with its cognate reductase subsequently catalyzes the oxidation of taxadiene to T5 $\alpha$ ol. The third enzyme, TAT, then catalyzes the acetylation of T5 $\alpha$ ol. Native, overexpressed genes are highlighted in blue whilst heterologous genes are highlighted in red. Dashed arrows highlight undesirable side-products; the structures of the two well-characterized by-products, OCT and iso-OCT are shown. GGPP, geranylgeranyl diphosphate; T5 $\alpha$ ol, taxadien-5 $\alpha$ -ol; TASY, taxadiene synthase; TAT, taxadien-5- $\alpha$ -ol O-acetyltransferase [Color figure can be viewed at [wileyonlinelibrary.com](http://wileyonlinelibrary.com)]



factories. State of the art micro and mini-bioreactor tools were subsequently employed to characterize and optimize the pathway for the production of oxygenated paclitaxel precursors across a range of scales for the first time. Design of experiment strategies was applied to rapidly determine the key factors affecting productivity at microscale, whilst minimizing time and resource costs. Optimal conditions were then validated using novel scale down benchtop bioreactors accelerating progress towards paclitaxel biosynthesis.

## 2 | MATERIALS AND METHODS

### 2.1 | Strain construction

The parent *S. cerevisiae* strain used in this study, LRS5 (*MATa*, *leu2-3, 112::HIS3MX6-GAL1p-ERG19/GAL10p-ERG8;ura3-52::URA3-GAL1p-MvaSA110G/GAL10p-MvaE* [codon optimized]; *his3Δ1::hphMX4-GAL1p-ERG12/GAL10p-IDI1*; *trp1-289::TRP1\_GAL1p-CrtE(X.den)/GAL10p-ERG-20;YPRCdelta15::NatMX-GAL1p-CrtE(opt)/GAL10p-CrtE*; *ARS1014::GAL-*

1p-TASY-GFP; ARS1622b::GAL1p-MBP-TASY-ERG20; ARS1114a::TDH-3p-MBP-TASY-ERG20) was originally derived from laboratory strain CEN.PK2-1C (EUROSCARF) and has been described in more detail elsewhere (Nowrouzi et al., 2020; Reider Apel et al., 2016). Strain LRS6 was constructed through the addition of gene sequences encoding CYP725A4, its cognate cytochrome P450 reductase (CPR) enzyme and TAT obtained from *Taxus cuspidata*. The synthetic genes were codon optimized for *S. cerevisiae* expression and synthesized by Integrated DNA Technologies. The resulting sequences, all required primers, and single-guide RNA (sgRNA) oligonucleotides were also synthesized by Integrated DNA Technologies. Chromosomal integration of transcriptional units was achieved using a cloning-free, Cas9-aided, homologous recombination method as reported by (Reider Apel et al., 2016). In summary, 2  $\mu$  plasmids expressing both Cas9 and the selected sgRNA were used. The URA3 selection marker, carried by the plasmid facilitated successful transformant selection on CSM-Ura medium agar plates. For verification of genomic integrations, Sanger sequencing (Edinburgh Genomics) and Next Generation Sequencing (NGS) were used. MinION NGS platform (Oxford Nanopore Technologies) was used for whole-genome sequencing along with the rapid library preparation kit, SQK-RAD004. Bioinformatics analysis was carried out by using pomoxis and medaka software and Python. The transformation was performed according to the LiAc/SS carrier DNA/PEG method (Gietz & Schiestl, 2007). All chemicals were purchased from Fisher Scientific at the highest available purity unless otherwise stated.

## 2.2 | Shake flask cultivations

The LRS6 strain was cultivated in 250 ml Erlenmeyer flasks for 3 days. Inocula preparation was achieved by transferring single colonies to 5 ml of rich YPD medium (1% yeast extract; 2% peptone; and 2% glucose) and incubating at 30°C and 250 rpm overnight. Aliquots of each preculture were subsequently diluted with YP supplemented with 2% galactose to yield a 20 ml culture with initial optical density (OD)<sub>600</sub> = 1. A 20% dodecane overlay was added to give a final working volume of 25 ml. Duplicate measurements of biomass were performed for triplicate shake flasks twice daily. Taxane production was analyzed via gas chromatography-mass spectrometry (GC-MS) at the end of the cultivation.

## 2.3 | Microscale high-throughput bioreactors

For the high-throughput screening, a BioLector Pro (mp2-labs) microbioreactor-screening platform was utilized. The microbial cultures were performed in triplicate in YP medium supplemented with one of eight sugar solutions (Table 1), each representing one of the conditions explored. Inocula were prepared as described for the shake flasks. Aliquots of the appropriate preculture were diluted eightfold to a volume of 800  $\mu$ l in each well with the medium indicated in the experimental design (Table S3). A 200- $\mu$ l dodecane

**TABLE 1** Media compositions investigated during high-throughput screening experiments

Total sugar concentration (%; w/v)	Yeast extract (g/L)	Peptone (g/L)	Ratio of glucose to galactose
2	10	20	0:100
2	10	20	10:90
2	10	20	50:50
4	10	20	0:100
4	10	20	10:90
4	10	20	50:50
0.2	10	20	10:90
0.4	10	20	10:90

overlay was also added to each well giving a total working volume of 1 ml. The temperature was maintained at 30°C under agitation of 1000 rpm with a shaking diameter of 3 mm in 48-well FlowerPlates (mp2-labs). Temperature, biomass, dissolved oxygen (DO), and pH were monitored online using the inbuilt optical sensors. Taxane production was analyzed via GC-MS at the end of the cultivation.

## 2.4 | Bioreactor conditions

Larger scale cultivations were conducted in MiniBio500 bioreactors (Applikon Biotechnology) with a working volume of 250 ml or 1 L BIOSTAT Q plus bioreactors (Sartorius-Stedim Biotech S.A.) with a working volume of 500 ml. Preinoculum cultures were prepared by transferring from a single colony to 5 ml of YPD and incubating at 30°C and 250 rpm for 8 h. The resulting culture was subsequently used to inoculate a secondary culture to an OD<sub>600</sub> = 1 and incubated overnight. An aliquot of the resulting culture was diluted with 2% (w/v) galactose medium to give a 200 (MiniBio 500) or 400 ml (BIOSTAT) culture with an initial OD<sub>600</sub> = 1.

To prevent excess foam production polypropylene glycol P2000 (Alfa Aesar) was added to a concentration of 0.01% (v/v) and a Rushton turbine was placed at the medium-air interface. A 20% dodecane overlay was also added. Temperature, DO, and pH were measured online. The adaptive my-control system (Applikon Biotechnology) was used to control process parameters in the MiniBio 500 bioreactors. A setpoint of 30% saturation for DO was applied and the culture temperature was maintained at 30°C. Where pH control was implemented, pH was maintained above six through the automatic addition of 1 M NaOH. Where biomass was measured online, a BE2100 OD scanner (BugLab) was employed, and offline measurements were performed twice daily using a Nanodrop 2000c spectrophotometer (Thermo Fisher Scientific). MFCS software (version 3.0, Sartorius-Stedim Biotech S.A.) was employed to control the BIOSTAT cultivation, pH was maintained at six through the automatic addition of 2 M NaOH or 2 M H<sub>2</sub>SO<sub>4</sub>, and temperature was

maintained at 30°C. A constant airflow of 1 vvm was maintained and stirrer speed was adjusted to maintain DO above 30%. Off-gas analysis was performed online via mass spectrometry (Prima Pro, Thermo Fisher Scientific). Samples were taken twice daily for taxane and metabolite quantification via GC-MS and high-performance liquid chromatography (HPLC).

## 2.5 | Taxane and metabolite identification and quantification

Taxane identification and quantification was achieved via GC-MS. The organic dodecane layer was separated from the culture medium through centrifugation and a 1- $\mu$ l sample was injected into a TRACE™ 1300 Gas Chromatograph (Thermo Fisher Scientific) coupled to an ISQ LT single quadrupole mass spectrometer (Thermo Fisher Scientific). Chromatographic separation was achieved using a Trace Gold TG-SQC gas chromatography column using a previously described method (Nowrouzi et al., 2020). To identify and quantify the production of compounds by *LRS5* and *LRS6* (Figure S1), pure standards of taxadiene, kindly supplied by Baran Lab (The Scripps Research Institute) and GGOH, obtained from Sigma Aldrich (Gillingham), were used. Additional product concentrations were estimated relative to standard taxadiene concentrations. In the BIOSTAT cultivation, ethanol, acetate, and glycerol production were analyzed via ion-exchange HPLC. Following filtration using a 0.45- $\mu$ m filter, 20- $\mu$ l samples were injected into a Bio-Rad Aminex HPX-87H column for analysis. The eluent was 5 mM H<sub>2</sub>SO<sub>4</sub>, flowrate 0.6 ml/min, and the temperature was 60°C. A RID-detector was used for quantification.

## 2.6 | Statistical analysis

Design of experiments and statistical analyses were performed using Minitab 17 statistical software. A balanced analysis of variance was used to determine whether investigated factors yielded a significant impact on measured variables in the microscale yeast cultures. The null hypothesis considered that there was no significant difference between the cultures, hence if  $p \leq .05$  the null hypothesis was

rejected. Pearson's correlation coefficient was used to assess linear relationships between variables.

## 3 | RESULTS AND DISCUSSION

### 3.1 | Strain construction

Taxadiene synthesis is the first committed step in the Taxol biosynthetic pathway and has been achieved in batch cultivation of *S. cerevisiae* with maximum taxadiene titers of 129 and 57 mg/L at 20°C and 30°C, respectively (Nowrouzi et al., 2020). The oxygenation step in the microbial host was achieved in this study through the chromosomal integration of *T. cuspidata* CYP725A4 and CPR genes in tandem into locus 511b. The TAT gene, also originating from *T. cuspidata*, was integrated into locus RKC3 to construct the subsequent acetylation step. In the native host genome, locus 511b is located in chr V: 175.892–175.911 on the forward strand, locus RKC3 is located in chr III: 119.278–119.313 on the forward strand and both of the loci are in intergenic regions. The GAL1 promoter was selected to maximize expression for both CYP725A4 and TAT. Expression of the CPR enzyme has been shown to be typically approximately 15-fold lower in its native host (Jensen & Møller, 2010), as disruption of the degree of coupling between the CPR and P450 enzymes increases the generation of toxic reactive oxygen species (Zangar et al., 2004). To minimize this effect, a single copy of CPR was expressed under the weaker GAL3 promoter. Zhou et al. (2015) highlighted the acetylation step by TAT to be the bottleneck of the early pathway, therefore the stronger GAL1 promoter was also selected for this gene as well as terminator CYC1. The construction of the genetic parts integrated into the chromosome of *LRS6* is shown in Figure 2.

### 3.2 | Shake flask cultivation performance and enzyme characterization

To facilitate preliminary product and growth profile characterization, the constructed *LRS6* strain was grown in shake flask cultures where the biomass kinetics and final product profile shown in Figure 3a.

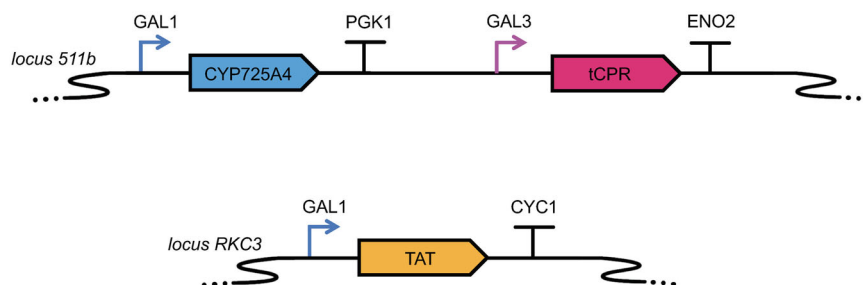


**FIGURE 2** Construction of T5 $\alpha$ Ac pathway in *Saccharomyces cerevisiae*. Genes CYP725A4 and CPR were chromosomally integrated in tandem into locus 511b to facilitate T5 $\alpha$ ol biosynthesis. TAT was subsequently integrated into locus RKC3 for the acetylation of T5 $\alpha$ ol to T5 $\alpha$ Ac. T5 $\alpha$ ol, taxadien-5 $\alpha$ -ol; TAT, taxadien-5- $\alpha$ -ol O-acetyltransferase [Color figure can be viewed at [wileyonlinelibrary.com](https://onlinelibrary.wiley.com/doi/10.1002/biot.27569)]



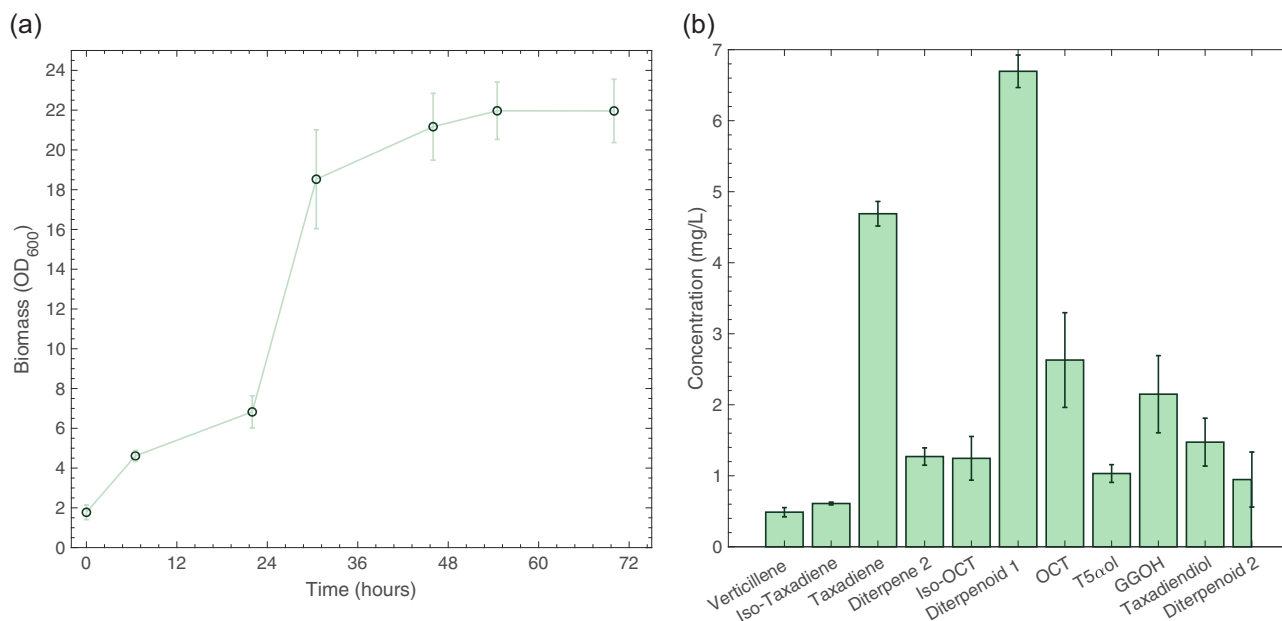


**FIGURE 3** LRS6 growth and productivity characterization in shake flasks. (a) Plot of biomass measured as absorbance at 600 nm. (b) Final Taxane and GGOH titers determined via gas chromatography-mass spectrometry. Values are mean  $\pm$  standard deviation for triplicate shake flasks [Color figure can be viewed at [wileyonlinelibrary.com](http://wileyonlinelibrary.com)]

Biomass accumulation by *LRS6* reached a final OD<sub>600</sub> of  $22.0 \pm 1.6$  after 71 h of culture, cultivation of the parent *LRS5* strain under the same experimental conditions resulted in a substantially higher OD<sub>600</sub> of  $36.0 \pm 1.8$  in just 48 h (Figure S2). In a similar previous study, *LRS5* biomass accumulation was also found to be 40% higher in shake flask culture (Nowrouzi et al., 2020). The reduced growth rate observed in the *LRS6* strain is therefore likely to be associated with the increased oxidative stress associated with the expression of the additional enzymes. A similar effect was observed when the *CYP725A4* and cognate *CPR* genes were incorporated into an optimized taxadiene-producing *E. coli* strain, biomass accumulation declined by over 50% (Ajikumar et al., 2010).

GC-MS analysis of the dodecane extracts from *LRS6* cultures in this study confirmed the functional expression of both the *TASY* and *CYP725A4* genes as shown in Figures 3a and S7a. A total of six oxygenated products were produced by the strain in addition to the *TASY* products. The peaks at 8.34, 8.57, and 8.71 min were identified as iso-OCT, OCT, and T5 $\alpha$ ol through comparison of the gas chromatographs and mass spectra (Figures S5 and S6) to those reported in the literature (Edgar et al., 2016; Sagwan-Barkdoll & Anterola, 2018). When expressed in *E. coli*, OCT and iso-OCT were previously found to be the major products of *CYP725A4* (Edgar et al., 2016; Sagwan-Barkdoll & Anterola, 2018; Yadav, 2014). In this study, however, a novel oxygenated diterpenoid with a retention time of 8.49 min (diterpenoid 1, Figure S7a) was the major product with a titer of  $7 \pm 0.2$  mg/L. The mass spectrum for this compound showed a high level of similarity to that of T5 $\alpha$ ol (Figure S5), suggesting isomerism, however, further characterization is necessary to confirm this. An additional unknown oxygenated diterpenoid compound was eluted after 10.03 min (diterpenoid 2, Figure S7a) with characteristic

peaks at  $m/z$  55, 105, 138, 273, and 288 (Figure S6). The *CYP725A4* enzyme, like many cytochrome P450 enzymes, has been shown to be multispecific in addition to highly promiscuous. The enzyme's activity on taxadiene, iso-taxadiene, and at least one mono-oxygenated taxane has been reported (Edgar et al., 2016; Jennewein et al., 2004; Yadav, 2014). An additional component was eluted at 9.41 min with a molecular ion ( $M^+$ ) peak ( $m/z$ ) of 304. This was equivalent to taxadiene ( $M_r = 272$  g/mol) plus  $O_2$  ( $M_r = 32$  g/mol) and was therefore tentatively identified as a taxadienol.

The nature of the majority of the side-products generated from *CYP725A4* was similar to those previously reported (Edgar et al., 2016; Sagwan-Barkdoll & Anterola, 2018; Yadav, 2014). However, the appearance and predominance of a potential T5 $\alpha$ ol isomer (diterpenoid 1) was novel. The expected TAT product, taxa-4(20),11-dien-5 $\alpha$ -yl acetate (T5 $\alpha$ Ac), was not detected. This was believed to be due to insufficient substrate availability as the maximum T5 $\alpha$ ol titer achieved under these conditions was just  $1 \pm 0.1$  mg/L. Subsequent experiments therefore focussed on the overproduction of the taxadiene and T5 $\alpha$ ol precursors.

### 3.3 | Microscale high throughput optimization

To maximize process insight and understanding, the BioLector Pro (mp2-labs) microbioreactor-screening platform was coupled with a design of experiments approach for the high-throughput screening of bioprocessing conditions. A multilevel full-factorial experiment was employed to analyze the effects of three key factors on taxane accumulation: yeast strain, total sugar concentration, and glucose content (Table S3). Both yeast strains were initially cultivated at two

different total sugar concentrations, 2% and 4%, to evaluate the effect of sugar concentration and overflow metabolism on the production of taxanes. As the overexpression of the native mevalonate pathway and heterologous expression of *TASY*, *CYP725A4*, *CPR*, and *TAT* relied on *GAL* promoters, the addition of galactose was required for taxane production. In this study, *LRS5* and *LRS6* were cultivated in pure galactose along with 10:90 and 50:50 mixtures of glucose and galactose to determine the optimum for biomass and taxane accumulation. The bioreactor results and final product profile of the high-throughput microscale screening are summarized in Figures 4 and 5, respectively.

### 3.3.1 | Microscale biomass kinetics

It can be clearly seen in Figure 4a that when sugar concentration was increased from 2% to 4% for the *TASY* strain (*LRS5*), a significant increase in final  $OD_{600}$  was observed from  $47.8 \pm 4.2$  to  $70.4 \pm 5.6$ , respectively. A similar effect was seen in the *LRS6* cultures; however, as in the shake flask cultivations (Figure 3), the final biomass

concentrations were lower than for the *LRS5* cultures, at  $42.3 \pm 1.3$  and  $54.3 \pm 7.2$  for 2% and 4% sugar cultures, respectively due to the expression of *CYP725A4*, *CPR*, and *TAT*. Supplementation of the cultures with glucose resulted in no significant improvement in final biomass yield for both strains under all conditions tested. As expected, the rate of growth for the pure galactose cultures was slower than that of equivalent glucose-containing cultures with a longer cultivation time being required to reach the stationary phase of growth.

### 3.3.2 | Taxane product profiles using microscale bioreactors

The *LRS5* strain produced a maximum taxadiene titer of  $137 \pm 5$  g/L when grown in 4% galactose (100:0) medium. This represented 1.06 and 2.5-fold improvements in taxadiene titer to  $137 \pm 5$  mg/L compared with the highest literature titers for the strain at 20 and 30°C (Nowrouzi et al., 2020). Although *TASY* activity has been found to be enhanced at reduced temperature (Nowrouzi et al., 2020), preliminary studies (results not shown) using *LRS6* revealed that

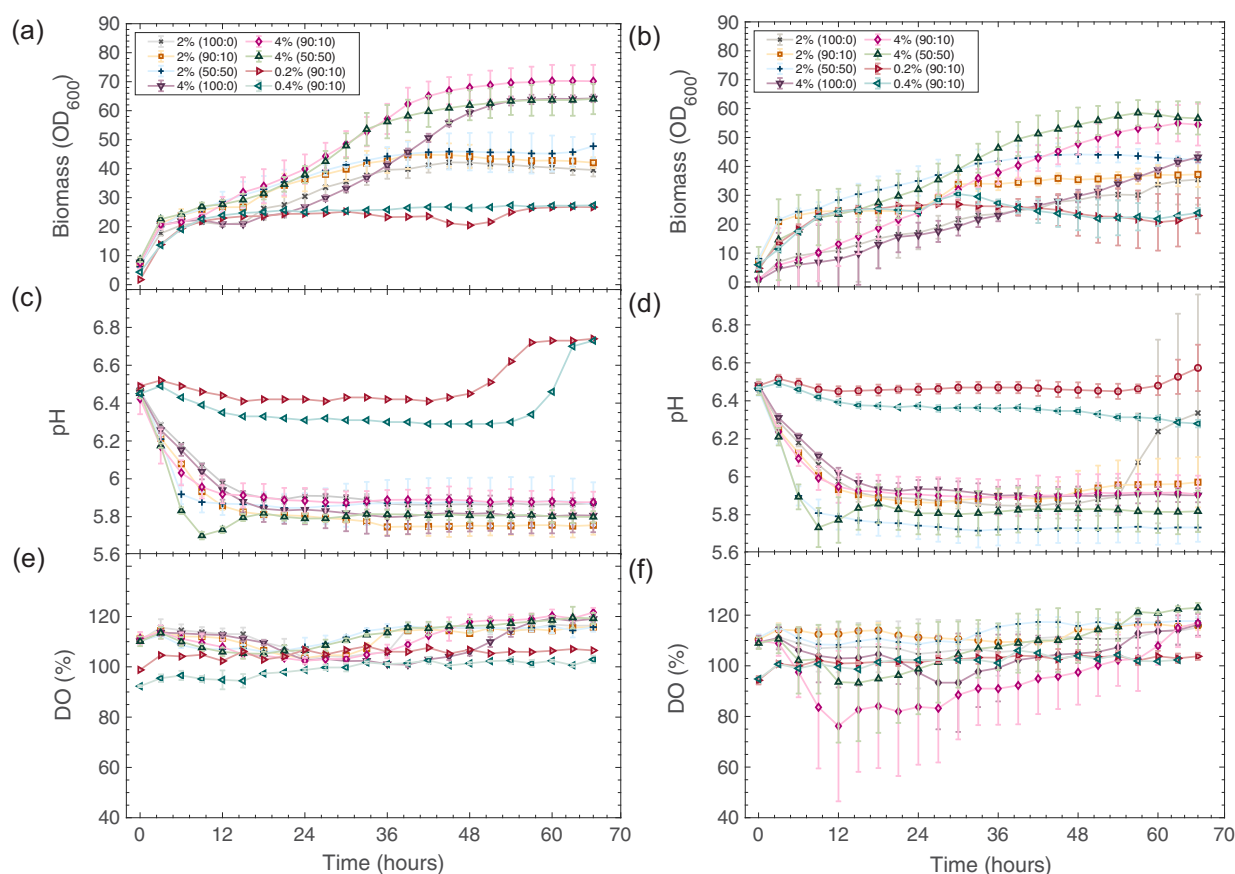


**FIGURE 4** Online high throughput microscale screening results. Plots on the left (a), (c), and (e) and right (b), (d), and (f) correspond to data from *LRS5* (*TASY* only) and *LRS6* (*TASY*, *CYP725A4*, *CPR*, and *TAT*) cultivations, respectively. Biomass concentration (a) and (b), pH (c) and (d), and DO concentration (e) and (f) were measured continuously in each well, values are mean  $\pm$  standard deviation for triplicate readings. Percentage values correspond to total sugar concentration (0.2%, 0.4%, 2%, or 4%) and values in parentheses correspond to galactose to glucose ratio. DO, dissolved oxygen; *TASY*, taxadiene synthase; *TAT*, taxadien-5- $\alpha$ -ol O-acetyltransferase [Color figure can be viewed at [wileyonlinelibrary.com](http://wileyonlinelibrary.com)]

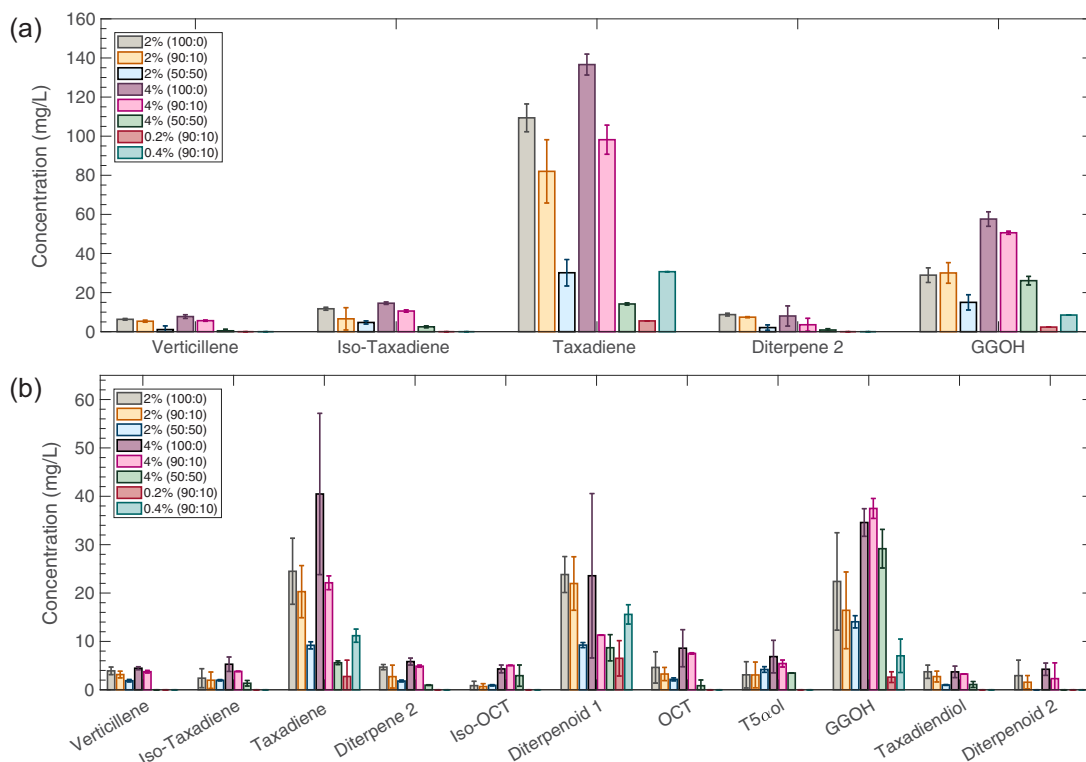


**FIGURE 5** Taxanes and GGOH production using microscale instrumentation by *LRS5* (a) and *LRS6* (b). Percentage values correspond to total sugar concentration (0.2%, 0.4%, 2%, or 4%) and values in parentheses correspond to galactose to glucose ratio. Values are mean  $\pm$  standard deviation for triplicate cultivations [Color figure can be viewed at [wileyonlinelibrary.com](https://onlinelibrary.wiley.com)]

CYP725A4 activity was dramatically reduced at 20°C compared with 30°C. In addition, both growth rate in *S. cerevisiae* (Nowrouzi et al., 2020) and CYP725A4 activity in *E. coli* (Biggs et al., 2016) have been found to be reduced at a lower temperature. This study, therefore, focussed on strategic optimization to ensure high taxadiene titers at 30°C. The highest concentration of oxygenated taxanes was also achieved for *LRS6* grown in the 4% galactose (100:0) medium at 51 mg/L, representing a 1.5-fold increase compared with the highest concentration reached using the *E. coli/S. cerevisiae* consortium system (Zhou et al., 2015). Although the qualitative nature of the *LRS6* taxane products was highly similar to those observed in the shake flask cultures, the quantitative product profiles differed considerably between the two scales which can be clearly seen in Figure S7a and S7c. Similar variations in CYP725A4 selectivity in response to changes in processing conditions, including microbial host, growth media, and extraction method have been observed previously (Edgar et al., 2016). An additional compound with a retention time of 9.28 min was observed in the optimal BioLector cultivation (Figures S7c and S8), showing a high degree of similarity to the published mass spectrum of geranylgeranyl acetate (GGAc; Walker et al., 1999). The endogenous GGOH side-product which was observed in this study has been previously shown to be a substrate of TAT, the product of which is GGAc. The presence of GGAc here indicated potential functional expression of TAT, however, the desired TAT product, T5 $\alpha$ Ac, was still not detected.

Mixed glucose and galactose carbon sources (2% [90:10]) have been previously found to enhance the production of an alternative heterologous isoprenoid, amorphadiene, in *S. cerevisiae*, (Paradise et al., 2008). However, in this study, it can be clearly seen in Figure 5a that increasing the glucose content generally hindered the production of the different oxygenated and nonoxygenated taxanes by both strains significantly. For example, when using *LRS5* with 2% (w/v) of carbon source with 10% and 50% of glucose content, the taxane titers declined by 28% and 90% in comparison with using pure galactose. A similar trend was observed when using 4% (w/v) of carbon source for the synthesis of oxygenated and nonoxygenated taxanes by *LRS5* and *LRS6*.

It was, therefore, concluded that pure galactose was the most appropriate carbon source for taxane production. This was expected as the GAL promoters are actively repressed by glucose and galactose is required for their induction. In addition, a reduction in overflow metabolism may have resulted from the slower growth rate of *S. cerevisiae* on galactose (Perez-Samper et al., 2018). As taxane production relies on products of aerobic respiration, this may also contribute to higher taxane titers, however, further research is required to confirm this. Increasing the initial sugar concentration from 0.4% to 2% galactose improved *LRS5* taxadiene titers 3.5-fold. However, when the initial concentration was doubled further to 4%, an increase in taxadiene titer of just 20% was obtained. The higher sugar concentration also favored the side reaction converting the



GGPP precursor to GGOH, the titer of which increased twofold when cultures were supplemented with 4% pure galactose in comparison with 2%. To maximize flux through the desired pathway and minimize undesirable endogenous product formation, the 2% pure galactose medium was selected for subsequent cultivations.

### 3.3.3 | Microscale pH kinetics

Fermenting yeasts typically acidify their growth medium through a combination of proton pumping, organic acid secretion as well as carbon dioxide evolution, and dissolution (M. G. Walker & Stewart, 2016). This effect was observed for the two *S. cerevisiae* strains of this study, as shown in Figure 4c,d, in cultivations supplemented with 2% or 4% sugar. Acidification occurred during the first 10 h and was most significant in the 2% and 4% 50:50 galactose to glucose mixtures where the pH dropped to  $5.9 \pm 0.07$  and  $5.7 \pm 0.02$ , respectively. This was expected as glucose is fermented at a faster rate than galactose by *S. cerevisiae* and organic acids such as acetic acid are secreted as side-products of fermentation (Martinez et al., 2014). Despite this, alteration of the sugar composition had no significant difference in the final pH values of the cultures supplemented with 2% or 4% sugar ( $p = .159$ ). Acidification was negligible for cultures supplemented with 0.2% or 0.4% sugar, likely due to reduced fermentative metabolism.

### 3.3.4 | Microscale dissolved oxygen kinetics

High DO concentrations (>80%) were observed throughout the cultivation for all conditions explored as shown in Figure 4e,f, indicating

excellent oxygen mass transfer. However, the use of organic solvents is not recommended with FlowerPlates (m2p-labs, 2019), as the degradation of the DO sensor could occur. As a result, further experiments were conducted without a dodecane overlay to characterize the effect. DO concentration readings for the cultures with and without the overlay were similar with between 87% and 96% DO being maintained throughout the cultivation (Figure S9). The high oxygen transfer rate observed was, therefore, likely due to the use of the novel baffled FlowerPlates, which have been found to improve  $k_L a$  values twofold at 800 rpm compared with traditional round well microtiter plates (Funke et al., 2009), eliminating oxygen limitation in *S. cerevisiae* cultures.

## 3.4 | Process validation

### 3.4.1 | Scale-up of optimal microscale conditions

During high throughput microscale screening, 2% pure galactose medium was deemed optimal for maximizing flux through the heterologous taxol pathway and minimizing undesirable endogenous product accumulation. A scale-up of this condition was subsequently performed to predict the industrial scale performance of *LRS6*. This was achieved using a 500-ml benchtop MiniBio 500 bioreactor (Applikon Biotechnology) with a total working volume of 250 ml, representing a 250-fold scale up. The results of this experiment are summarized in Figure 6.

The total taxane product titers at micro and minibioreactor scale were highly similar at  $95 \pm 18$  and  $99$  mg/L, respectively. However, the final concentration of the potential T5 $\alpha$ l isomer was reduced substantially from  $24 \pm 4$  at microscale to  $9$  mg/L using the

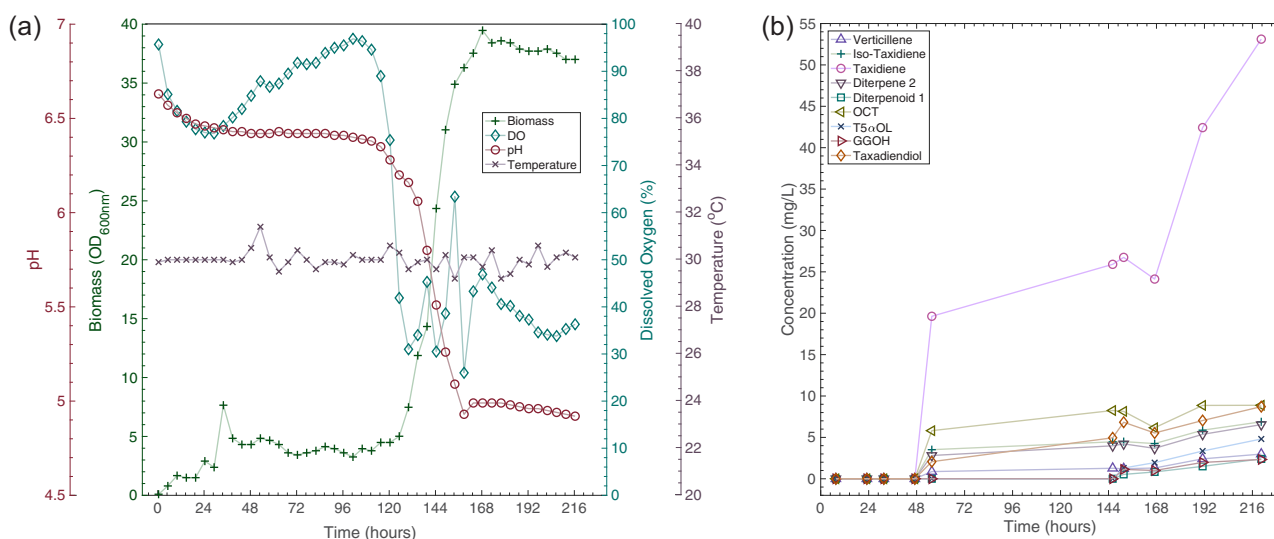


**FIGURE 6** Initial bioreactor cultivation results. *Saccharomyces cerevisiae* strain *LRS6* was cultivated in the Applikon MiniBio 500 bioreactors in 2% (100:0) medium. (a) Online process monitoring. Temperature and DO were monitored and controlled to set points of 30°C and 30%, respectively. Medium pH was also monitored online. (b) Taxane and GGOH concentration. DO, dissolved oxygen [Color figure can be viewed at [wileyonlinelibrary.com](http://wileyonlinelibrary.com)]

minibioreactor. Oxygenated taxane compounds accounted for just 21% of the total products in the bioreactor compared with  $41 \pm 4\%$  at microscale. Although acidification was observed in the microscale cultivations as shown in Figure 4c,d, it was much more significant in the bioreactor cultivation (Figure 6a). This likely contributed to the poor performance observed for the synthesis of oxygenated taxanes, as the optimal pH for the membrane-bound CYP725A4 has been reported to be 7.2 in its natural source, with activity dropping by 50% at pH 6.2 (Hefner et al., 1996). This may have been further exacerbated by the instability of NADPH at reduced pH, the rate of degradation of which increases as the pH decreases below 7.5, reducing electron availability, and potentially the activity of the reductase enzyme (Wu et al., 1986). According to a study by (Valli et al., 2005), the internal pH of *S. cerevisiae* varies with external pH. For exponentially growing cells cultivated in media buffered to pH 5.0 and 7.0, the internal pH values were around 6.3 and 7.1, respectively (Valli et al., 2005). The pH of the culture decreased from 6.6 to 4.9, suggesting that the internal pH likely dropped below 6.3. Whereas in the microscale cultures, the minimum external pH was  $5.9 \pm 0.1$  corresponding to an internal pH of approximately 6.7. The significant drop in pH observed in the bioreactor could therefore likely be responsible for the dramatic reduction in CYP725A4 activity. As a result, pH control was deemed necessary in future runs.

The  $OD_{600}$  plateaued at 37.0 ( $\sim 6.72$  g/L) in the stationary phase of growth as shown in Figure 6a, this was similar to the final value of

$35.5 \pm 8.7$  ( $\sim 6.44 \pm 1.58$  g/L) obtained for the same medium in the microscale bioreactor (Figure 4b). The ability of the BioLector to effectively mimic larger-scale cultivation performance has been demonstrated previously by Back et al., (2016). Although oxygenated taxane titers were lower at bioreactor scale in the study, biomass and total taxane concentrations were highly comparable.

### 3.4.2 | Effect of external pH

Although *S. cerevisiae* is capable of proliferating across a broad pH range, its growth rate is optimal between pH 4–6 (Narendranath & Power, 2005) and is decreased substantially above pH 8 (Peña et al., 2015). As there was a significant difference in optimal pH for the enzyme and host, an additional microscale study was conducted to evaluate the effect of pH on both taxane and biomass accumulation by *LRS6* as shown in Figure 7a,b.

The initial pH of the culture medium was buffered to seven through the addition of potassium buffer, which had a negative effect on both biomass and taxane accumulation. The final  $OD_{600}$  was  $15.8 \pm 2.2$  compared with  $37.1 \pm 4.4$  without the buffer as shown in Figure 7a. The titers of taxadiene and novel oxygenated diterpenoid 1 were also considerably lower at  $4 \pm 2$  and  $6 \pm 2$  mg/L compared with  $20 \pm 5$  and  $22 \pm 6$  mg/L for the nonbuffered cultures. The preliminary bioreactor results (Figure 6) indicated that although lower

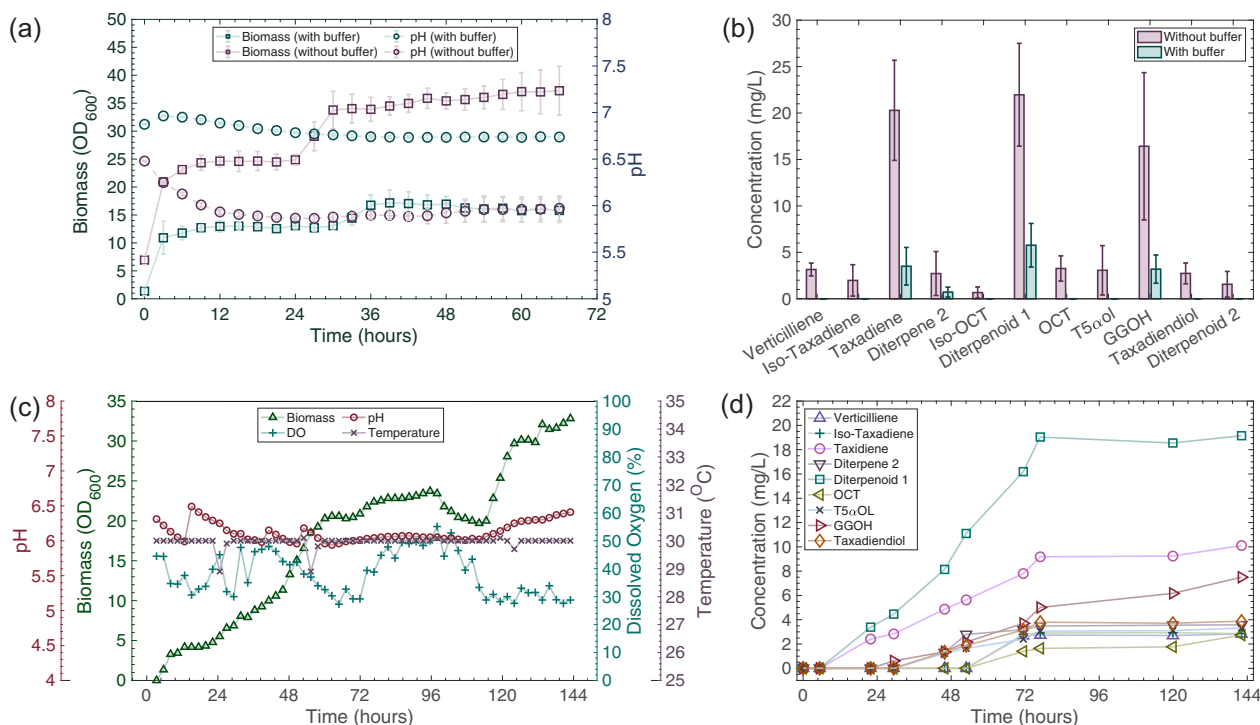


**FIGURE 7** Effect of medium pH on *LRS6* at micro and minibioreactor scale. (a) *LRS6* was cultivated in 2% (90:10) medium, both in the presence and absence of a pH 7 buffer (3 g/L potassium dihydrogen phosphate and 7 g/L disodium phosphate) in FlowerPlates at microscale. Values are mean  $\pm$  standard deviation for triplicate cultivations. (c) *LRS6* was cultivated in the Applikon MiniBio 500 bioreactors in 2% (100:0) medium. Temperature, pH, and DO were monitored online and controlled to set points of 30°C, 6% and 30%, respectively. DO, dissolved oxygen [Color figure can be viewed at [wileyonlinelibrary.com](http://wileyonlinelibrary.com)]

pH (<5.0) did not impair cell growth, it was detrimental to CYP725A4 activity. Higher pH (>6.5) hindered yeast growth and also led to lower oxygenated taxane titers. Although temporal monitoring of taxane accumulation was not possible at microscale due to limited culture volumes, statistical analysis of the MiniBio scale kinetics revealed a strong positive correlation between OD<sub>600</sub> and taxane titer (Pearson's  $r = .8916$ , Figure 6). A compromise was therefore necessary to maximize both taxane and biomass accumulation. The non-buffered culture dropped to around pH 6.0 as shown in Figure 7a and resulted in significantly higher total taxane titers. In addition, pH 6.0 has been shown to be the upper limit of the optimal range for yeast growth (Narendranath & Power, 2005). A pH of 6.0 was, therefore, implemented in the subsequent bioreactor cultivation, the data for which is summarized in Figure 7c,d. During the first 12 h of cultivation, a fivefold increase in biomass was observed, followed by a lag phase in the subsequent 12 h. A similar effect was observed in the shake flask (Figure 3a) and microscale cultures (Figure 4). This lag phase is characteristic of *S. cerevisiae* cultures as the carbon source is switched from glucose to galactose. The growth observed in the initial 12 h is, therefore, likely to have been the result of an additional, more preferable carbon source within the growth medium such as residual glucose from the inoculum or carbohydrates present in the complex yeast extract medium. The final OD<sub>600</sub> values for the initial cultivation without pH control (Figure 6a) and subsequent controlled cultivation (Figure 7c) were comparable at 38.9 and 34.5, respectively. When the pH was controlled above six in the mini-bioreactor (Figure 7d), the total product titer was 50% lower (56.0 mg/L) than that obtained in the absence of pH control (98.9 mg/L, Figure 6b). Despite this, the titer of diterpenoid 1 increased significantly from 8.9 (Figures 6b) to 19.2 mg/L (Figure 7d), confirming increased CYP725A4 activity at higher pH. Statistical analysis confirmed a strong positive correlation between total taxane concentration and OD<sub>600</sub> in the pH-controlled bioreactor (Pearson's  $r = .9625$ ). A pH of 6 was therefore selected for subsequent cultivations to maximize accumulation of both. This highlights the importance of integrating critical process parameter control in the early stages of the design-build-test-learn cycle to ensure effective microbial cell factory construction and optimization.

### 3.4.3 | Detection of taxadien-5 $\alpha$ -yl-acetate

GGAc was detected during the microscale optimization study, indicating potential TAT activity, however, it was not detected in the bioreactor or shake flask cultures. TAT relies on acetyl-CoA as a substrate, a major product of aerobic respiration. One of the key advantages of the baffled FlowerPlates employed in the microscale optimization study is excellent oxygen mass transfer (m2p-labs, 2019), which eliminated oxygen limitation. Although DO was controlled above 30% saturation through air sparging in the bioreactor, oxygen availability was likely reduced compared to the FlowerPlate. As galactose metabolism is respiratory-fermentative, it was hypothesized that increasing oxygen availability through constant

airflow at bioreactor scale may increase flux through aerobic respiration and hence acetylated taxane production. The optimized conditions were scaled up further using highly instrumented 1 L BIOSTAT bioreactors, with a constant airflow of 1 vvm, to facilitate further characterization. The results of this experiment are summarized in Figure 8.

As in previous cultivations an initial growth phase was observed. During the first 22 h of growth the OD<sub>600</sub> increased from 1 to 14.4 (Figure 8a). Following this a lag phase was observed and ethanol production initiated. At around 48 h, the ethanol concentration reached a maximum of 2.7 g/L (Figure 8a) and the oxygen uptake rate began to increase (Figure 8c). This indicated a switch from predominantly fermentative metabolism of galactose to aerobic respiration. Growth proceeded via respiration of ethanol and acetate with a maximum OD<sub>600</sub> of 34.6 (~6.28 g/L) being reached at around 72 h, highly comparable with the 34.5 (~6.26 g/L) obtained in the 500 ml bioreactor (Figure 7c). The rate of biomass and taxane accumulation was greatest between 48 and 72 h. At 72 h the metabolizable carbon sources, galactose, ethanol, and acetate had been exhausted and the stationary phase of growth was reached (Figure 8a). In the final 48 h of cultivation, a slight increase in total taxane concentration from 154 to 171 mg/L was observed despite the cells being in the stationary phase of growth. Previous work indicated that some taxadiene may be retained intracellularly and secreted during the stationary phase of growth (Nowrouzi et al., 2020). The observed increase in taxane concentration may have, therefore been the result of secreted intracellular taxanes. An alternative extraction procedure incorporating a cell lysis step could, therefore allow similar titers to be achieved in a shorter cultivation time.

Closer inspection of the mass spectrum of the suspected taxadienol compound produced in previous cultivations (Figure S6c) revealed peaks at  $m/z = 255, 270,$  and  $287$  in addition to the characteristic taxadienol peaks at  $m/z = 286$  and  $304$ . These peaks have not been reported in other taxadienol mass spectra, however, such peaks have been found diagnostic of T5 $\alpha$ Ac ( $255: P^+ \cdot CH_3COOH \cdot CH_3,$   $270: P^+ \cdot CH_3COOH,$  and  $287: P^+ \cdot CH_3CO;$  Walker et al., 1999). It was, therefore, further hypothesized that the two compounds may be coeluting. According to the fundamental resolution equation, increasing the length of the chromatography column generally improves separation, therefore, in this study, a 30-m column was used in place of the 15-m column used in previous results. This successfully improved chromatographic separation as shown in Figure S10b. An additional four potential diterpene and two potential diterpenoid compounds were detected (Figures S10b and S13). The taxadienol peak was successfully separated into two peaks with retention times of 11.89 and 11.91, respectively, however, there was overlapping observed indicating resolution could be improved further. The mass spectrum of the compound eluted at 11.89 min (Figure S11) was almost identical to that of T5 $\alpha$ Ac published in literature (Edgar et al., 2016; Walker et al., 1999) with the exception of a peak at  $m/z = 245$ . The peak at 11.91 contained the diagnostic taxadienol peaks at  $m/z = 304$  and  $286$  along with a large base peak at  $m/z = 245$

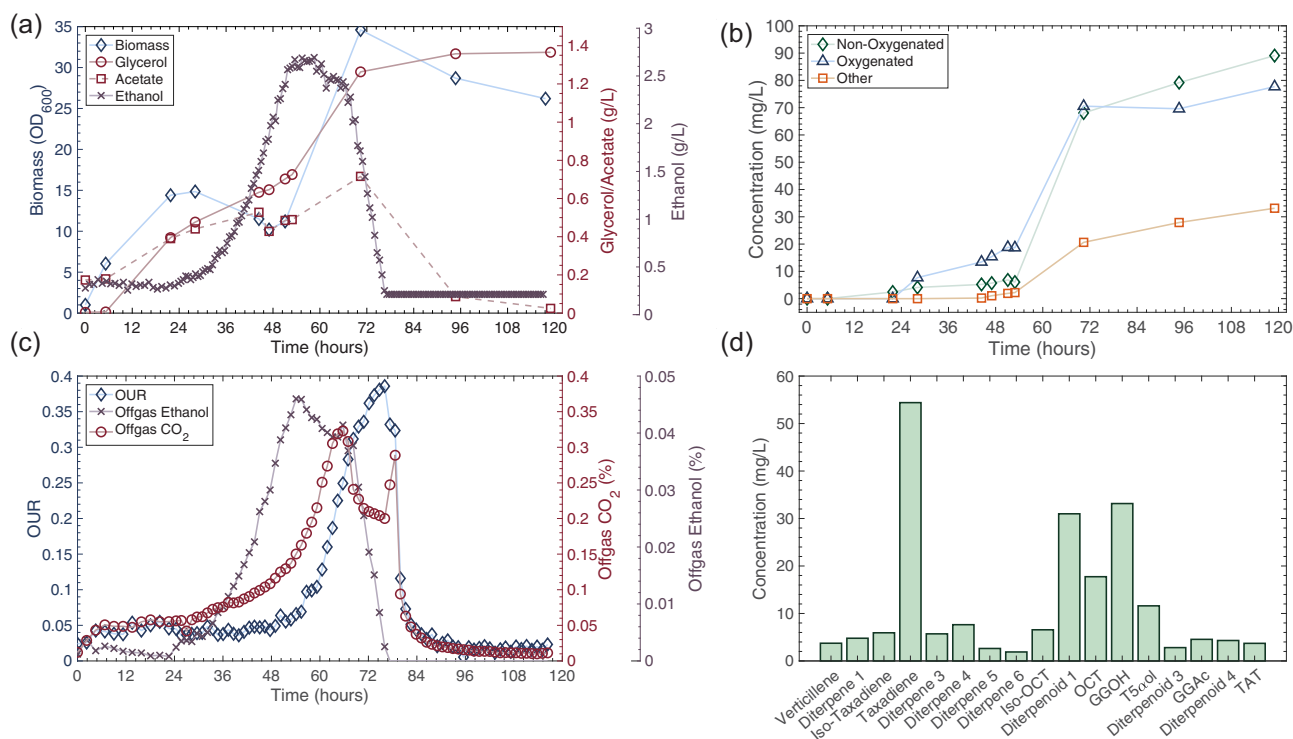


**FIGURE 8** Characterization in highly instrumented 1L BIostat bioreactors. *LRS6* was cultivated in the Applikon 1 L BIostat bioreactor in 2% (100:0) medium. (a) Biomass, ethanol, acetate, and glycerol concentration. (b) Taxane accumulation kinetic summary. Nonoxygenated products included verticillene, iso-taxadiene, taxadiene, diterpene 2, and the additional unknown diterpenes. Oxygenated products included iso-OCT, diterpenoid 1, 3, and 4, OCT, T5αol, and T5αAc. (c) Offgas analysis summary. Oxygen uptake rate (OUR) along with ethanol and CO<sub>2</sub> concentration was measured in the offgas online. (d) Final titer of each of the taxane products [Color figure can be viewed at [wileyonlinelibrary.com](http://wileyonlinelibrary.com)]

(Figure S12). An extracted ion chromatogram was generated for  $m/z = 245$ , this revealed a large single peak at 11.91 min (Figure S10a). This indicated that the peak at  $m/z = 245$  was most likely the result of overlapping rather than the compound eluted at 11.89 min. The compound eluted at 11.89 min was, therefore, tentatively identified as T5αAc. Quantification was performed relative to the taxadiene standard and the resulting final T5αAc titer was 3.7 mg/L, representing a fourfold improvement in acetylated taxadiene in *S. cerevisiae* in comparison with the previous literature (Zhou et al., 2015). Diterpene 2 was not detected using the optimized GC-MS protocol, however, an additional four diterpene compounds (diterpene 3, diterpene 4, diterpene 5, and diterpene 6, Figure S10b) were detected between taxadiene and iso-OCT. This suggests that the previously identified diterpene 2 compound may have also been two or more of the additional diterpene products coeluting.

### 3.5 | Comparison of the systems studied

The simultaneous expression of *TASY*, *CYP725A4*, *CPR*, and *TAT* was found to be sensitive to deviations in processing conditions at different production scales. Variations in both the titer and product composition were observed as summarized in Figures 9 and S7. The results obtained using the BioLector and uncontrolled MiniBio 500

systems were highly comparable for the *LRS6* strain. The final OD<sub>600</sub> values were  $42.3 \pm 1.3$  ( $\sim 7.68 \pm 0.24$  g/L) and  $38.9$  ( $\sim 7.06$  g/L), and the total product titers were  $95 \pm 18$  and  $99$  mg/L for the micro and minibioreactor systems, respectively. However, both oxygenated taxane and GGOH production were reduced in the bioreactor cultivation. The *CYP725A4* enzyme was found to be very sensitive to deviations in process conditions between the two scales. To compare selectivity across the systems studied, the yield of each product as a percentage of the total products was plotted as shown in Figure 9a. The total nonoxygenated and oxygenated taxane titers were also plotted in Figure 9b. The products of most interest were iso-taxadiene, taxadiene, diterpenoid 1, T5αol, and T5αAc, due to their active role in the Taxol biosynthetic pathway. Variation in selectivity towards these compounds across scales was, therefore also summarized in Figure 9c.

The major products of *TASY* and *CYP725A4* were found to be taxadiene and the novel potential T5αol isomer, diterpenoid 1, respectively, under all of the conditions explored. However, selectivity towards the minor enzymatic products varied considerably, with varying quantities of the additional side-products of the enzymes being produced as shown in Figure 9. Although the BioLector facilitated the monitoring of critical process parameters including pH and DO, control of such parameters was not practicable. This was particularly problematic for strain *LRS6* as

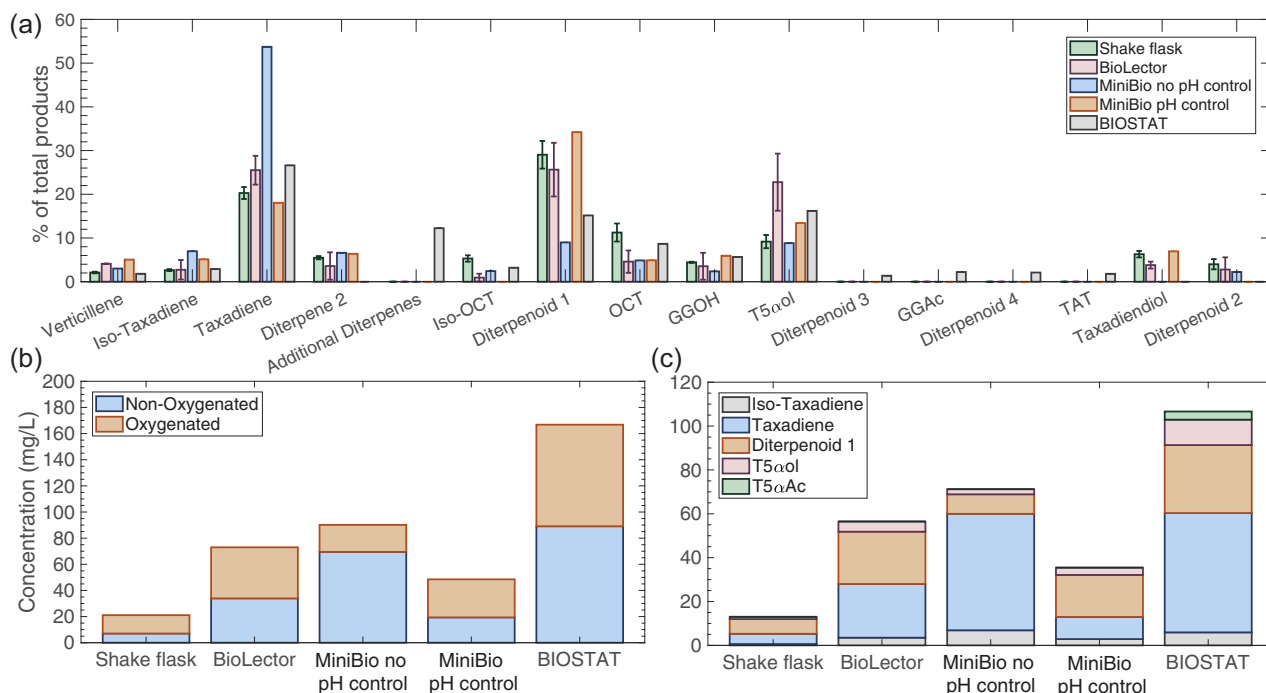


**FIGURE 9** Selectivity of engineered taxadien-5 $\alpha$ -ol biosynthetic pathway in *Saccharomyces cerevisiae* across a range of scales and bioprocessing conditions. (a) Yield of each product as a percentage of the total products. (b) Actual nonoxygenated and oxygenated taxane titers for each processing condition studied. Nonoxygenated products include verticillene, iso-taxadiene, taxadiene, diterpene 2, and the additional unknown diterpenes. Oxygenated products are iso-OCT, diterpenoid 1, 2, 3, and 4, OCT, T5 $\alpha$ ol, taxadiendiol, and T5 $\alpha$ Ac. (c) Actual titers of key taxol intermediates for each processing condition studied. *LR56* was cultivated at four scales, shake flask (25 ml), micro (1 ml), MiniBio 500 (250 ml), and BIOSTAT (500 ml). Bioreactor cultivations without and with pH control were performed [Color figure can be viewed at [wileyonlinelibrary.com](http://wileyonlinelibrary.com)]

CYP725A4 activity was found to be negatively affected by sub-optimal pH. Increased acidification in the uncontrolled bioreactor cultivation resulted in a 50% reduction in oxygenated taxane titer as shown in Figure 9b, despite highly comparable overall taxane titers. Although controlling the pH to a setpoint of 6 improved oxygenated taxane titers dramatically in subsequent cultivations, the final taxadiene titers were 10 and 54 mg/L for the pH-controlled MiniBio and BIOSTAT cultivations, respectively, indicating that CYP725A4 activity could be improved further. As the enzyme performs optimally at higher pH, increasing the pH of the culture medium in the final stages of the cultivation may improve conversion of taxadiene to T5 $\alpha$ ol; however, further research is required to confirm this. A small quantity of GGAc was detected in the BioLector cultivations indicating functional TAT expression. Through a combination of bioprocess optimization and improved GC-MS resolution at increased scale it was possible to detect the desired T5 $\alpha$ Ac compound. The resulting cultivation incorporated the optimized 2% galactose medium, pH setpoint of 6, and constant air supply at 1 vvm leading to a maximum titer of 3.7 mg/L. The oxygenated taxane titer was also improved 2.4-fold to 78 mg/L compared with the highest reported titer for the *E. coli*/*S. cerevisiae* consortium system (Zhou et al., 2015). To our knowledge, this is the first time acetylated taxanes have been successfully produced in an individual *S. cerevisiae* strain.

## 4 | CONCLUSION

In this study, critical factors affecting CYP725A4 enzymatic performance in an engineered *S. cerevisiae* strain were elucidated across a range of scales, providing a foundation for the development of robust integrated bioprocess control systems. Optimized cultivation of the engineered *S. cerevisiae* strain with three copies of taxadiene synthase (*LR55*) in the FlowerPlates facilitated 1.06 and 2.5-fold improvements in taxadiene titer to  $137 \pm 5$  g/L compared with the highest literature titers for the strain at 20 and 30°C (Nowrouzi et al., 2020). In this study, strategic optimization ensured high taxadiene titers at 30°C, thereby eliminating reliance on suboptimal cultivation temperatures. In contrast to bacterial systems in which the by-products OCT and Iso-OCT were the major products of CY725A4 (Edgar et al., 2016), when expressed in the *S. cerevisiae* strain, a novel potential T5 $\alpha$ ol isomer (diterpenoid 1) was the predominant product with maximum titers of  $24 \pm 6$  and 31 mg/L at micro and 1 L bioreactor scale, respectively. Biomass and total taxane titers achieved using the BioLector were comparable with those achieved in the MiniBio 500 bioreactor. The online monitoring capabilities of the BioLector proved invaluable for the primary high-throughput screening of wide-ranging processing conditions. However, as a result of the vulnerability of the complex cytochrome P450 enzyme to deviations in external processing conditions, further optimization



was essential to achieve comparable performance at an increased scale. Significant discrepancies were identified between the optimal conditions for the host and the catalytic activity of the different recombinant enzymes; therefore, a compromise was necessary to alleviate the key bottlenecks. Despite a 500-fold scale up in working volume, through careful control of critical process parameters including pH and  $O_2$ , paclitaxel precursor synthesis was improved substantially at bioreactor scale in just three experimental runs. Total oxygenated taxane titers were improved twofold to 78 mg/L and the acetylated T5 $\alpha$ Ac product was detected for the first time with a final titer of 3.7 mg/L. This highlights that maximizing process insight from the earliest stages of the design-build-test-learn cycle is critical to successful bioprocess development.

## ACKNOWLEDGMENTS

The authors would like to thank Ms. Caroline Delahoyde and Mr. Martin Corcoran at The School of Engineering, University of Edinburgh, UK and Dr Aaron John Christian Andersen and Mette Amfelt at the DTU Metabolomics Core, DTU, Denmark for their kind assistance and technical support with GC-MS analysis. Thanks to Tina Johansen at the DTU Fermentation Core, DTU, Denmark for her assistance with the BIOSTAT cultivations and HPLC analyses. Thanks to Professor Phil Baran's Lab at The Scripps Research Institute, San Diego, California for providing the taxadiene standard. This research was conducted with material produced with the assistance of the Edinburgh Genome Foundry, a synthetic biology research facility specialising in the assembly of large DNA fragments at the University of Edinburgh. This work was supported by the Engineering and Physical Sciences Research Council (Grant number EP/R513209/1), Ministry of National Education of the Republic of Turkey, The University of Edinburgh (Principal's Career Development PhD Scholarship), the Royal Society (Grant Number RSG\R1\180345), The University of Edinburgh Global Challenges Theme Development Fund 418 (Grant Number: TDF\_03), the US National Science Foundation (Award Number 1330914), and the Novo Nordisk Foundation within the frame of the Fermentation Based Biomanufacturing initiative (Grant Number: NNF17SA0031362).

## CONFLICT OF INTERESTS

Jay D. Keasling has financial interests in Amyris, Lygos, Demetrix, Napigen, Maple Bio, Apertor Labs, Ansa Biotechnologies, and Berkeley Brewing Sciences.

## AUTHOR CONTRIBUTIONS

Laura E. Walls designed and performed the majority of the shake flask, microscale and bioreactor experiments including all of the data analysis. Laura E. Walls wrote the manuscript with input from all authors. Jeff Wong, Leo d'Espaux and Rachel A. Li contributed with the genome engineering experiments. Behnaz Nowrouzi and Jonathan A. Dennis contributed with preliminary microscale and shake flask experiments. Koray Malcı contributed with the next generation sequencing experiments. Andrea J. C. Semião provided support with GC-MS analysis and reviewing the manuscript. Stephen

Wallace assisted with mass spectrometry analysis and reviewing the manuscript. José L. Martinez, Jay D. Keasling, and Leonardo Rios-Solis conceived and coordinated the study.

## DATA AVAILABILITY STATEMENT

The data that support the findings of this study are available from the corresponding author upon reasonable request.

## ORCID

Laura E. Walls  <http://orcid.org/0000-0002-9379-3593>

## REFERENCES

- Ajikumar, P. K., Xiao, W.-H., Tyo, K. E. J., Wang, Y., Simeon, F., Leonard, E., Mucha, O., Phon, T. H., Pfeifer, B., & Stephanopoulos, G. (2010). Isoprenoid pathway optimization for Taxol precursor overproduction in *Escherichia coli*. *Science*, 330(6000), 70–74. <https://doi.org/10.1126/science.1191652>
- Back, A., Rossignol, T., Krier, F., Nicaud, J.-M., & Dhulster, P. (2016). High-throughput fermentation screening for the yeast *Yarrowia lipolytica* with real-time monitoring of biomass and lipid production. *Microbial Cell Factories*, 15(1), 147. <https://doi.org/10.1186/s12934-016-0546-z>
- Biggs, B. W., Lim, C. G., Sagliani, K., Shankar, S., Stephanopoulos, G., De Mey, M., & Ajikumar, P. K. (2016). Overcoming heterologous protein interdependency to optimize P450-mediated Taxol precursor synthesis in *Escherichia coli*. *Proceedings of the National Academy of Sciences of the United States of America*, 113(12), 3209–3214. <https://doi.org/10.1073/pnas.1515826113>
- DeJong, J. M., Liu, Y., Bollon, A. P., Long, R. M., Jennewein, S., Williams, D., & Croteau, R. B. (2006). Genetic engineering of taxol biosynthetic genes in *Saccharomyces cerevisiae*. *Biotechnology and Bioengineering*, 93(2), 212–224. <https://doi.org/10.1002/bit.20694>
- Doran, P. M. (1995). Bioprocess development: An interdisciplinary challenge. In P. M. Doran (Ed.), *Biochemical engineering* (2nd ed.). Academic Press. <https://doi.org/10.1016/B978-012220855-3/50001-8>
- Edgar, S., Zhou, K., Qiao, K., King, J. R., Simpson, J. H., & Stephanopoulos, G. (2016). Mechanistic Insights into taxadiene epoxidation by taxadiene-5 $\alpha$ -hydroxylase. *ACS Chemical Biology*, 11(2), 460–469. <https://doi.org/10.1021/acscchembio.5b00767>
- Engels, B., Dahm, P., & Jennewein, S. (2008). Metabolic engineering of taxadiene biosynthesis in yeast as a first step towards Taxol (Paclitaxel) production. *Metabolic Engineering*, 10(3-4), 201–206. <https://doi.org/10.1016/j.ymben.2008.03.001>
- Funke, M., Buchenauer, A., Schnakenberg, U., Mokwa, W., Diederichs, S., Mertens, A., Müller, C., Kensy, F., & Büchs, J. (2010). Microfluidic bioreactor—microfluidic bioprocess control in microtiter plates. *Biotechnology and Bioengineering*, 107(3), 497–505. <https://doi.org/10.1002/bit.22825>
- Funke, M., Diederichs, S., Kensy, F., Müller, C., & Büchs, J. (2009). The baffled microtiter plate: Increased oxygen transfer and improved online monitoring in small scale fermentations. *Biotechnology and Bioengineering*, 103(6), 1118–1128. <https://doi.org/10.1002/bit.22341>
- Gietz, R. D., & Schiestl, R. H. (2007). High-efficiency yeast transformation using the LiAc/SS carrier DNA/PEG method. *Nature Protocols*, 2, 31–34. <https://doi.org/10.1038/nprot.2007.13>
- Hefner, J., Rubenstein, S. M., Ketchum, R. E. B., Gibson, D. M., Williams, R. M., & Croteau, R. (1996). Cytochrome P450-catalyzed hydroxylation of taxa-4(5),11(12)-diene to taxa-4(20),11(12)-dien-5 $\alpha$ -o1: The first oxygenation step in taxol biosynthesis. *Chemistry & Biology*, 3(6), 479–489. [https://doi.org/10.1016/S1074-5521\(96\)90096-4](https://doi.org/10.1016/S1074-5521(96)90096-4)
- Jennewein, S., Long, R. M., Williams, R. M., & Croteau, R. (2004). Cytochrome P450 taxadiene 5 $\alpha$ -hydroxylase, a mechanistically

- unusual monooxygenase catalyzing the first oxygenation step of taxol biosynthesis. *Chemistry & Biology*, 11(3), 379–387. <https://doi.org/10.1016/j.chembiol.2004.02.022>
- Jensen, K., & Møller, B. L. (2010). Plant NADPH-cytochrome P450 oxidoreductases. *Phytochemistry*, 71(2), 132–141. <https://doi.org/10.1016/j.phytochem.2009.10.017>
- Kensy, F., Zang, E., Faulhammer, C., Tan, R.-K., & Büchs, J. (2009). Validation of a high-throughput fermentation system based on online monitoring of biomass and fluorescence in continuously shaken microtiter plates. *Microbial Cell Factories*, 8, 31. <https://doi.org/10.1186/1475-2859-8-31>
- Kostov, Y., Harms, P., Randers-Eichhorn, L., & Rao, G. (2001). Low-cost microbioreactor for high-throughput bioprocessing. *Biotechnology and Bioengineering*, 72(3), 346–352. [https://doi.org/10.1002/1097-0290\(20010205\)72:3<346::AID-BIT12>3.0.CO;2-X](https://doi.org/10.1002/1097-0290(20010205)72:3<346::AID-BIT12>3.0.CO;2-X)
- Liu, W. C., Gong, T., & Zhu, P. (2016). Advances in exploring alternative Taxol sources. *RSC Advances*, 6(54), 48800–48809. <https://doi.org/10.1039/C6RA06640B>
- m2p-labs. (2019). FlowerPlate - Data sheet Flowerplate.
- Martínez, J. L., Bordel, S., Hong, K.-K., & Nielsen, J. (2014). Gcn4p and the Crabtree effect of yeast: Drawing the causal model of the Crabtree effect in *Saccharomyces cerevisiae* and explaining evolutionary trade-offs of adaptation to galactose through systems biology. *FEMS Yeast Research*, 14(4), 654–662. <https://doi.org/10.1111/1567-1364.12153>
- McElroy, C., & Jennewein, S. (2018). Taxol<sup>®</sup> biosynthesis and production: From forests to fermenters. In W. Schwab, B. M. Lange, & M. Wüst (Eds.), *Biotechnology and natural products* (pp. 145–185). Springer International Publishing. [https://doi.org/10.1007/978-3-319-67903-7\\_7](https://doi.org/10.1007/978-3-319-67903-7_7)
- Narendranath, N. V., & Power, R. (2005). Relationship between pH and medium dissolved solids in terms of growth and metabolism of lactobacilli and *Saccharomyces cerevisiae* during ethanol production. *Applied and Environmental Microbiology*, 71(5), 2239–2243. <https://doi.org/10.1128/AEM.71.5.2239-2243.2005>
- Nowrouzi, B., Li, R., Walls, L. E., d'Espaux, L., Malci, K., Liang, L., Borrego, N. J., Lerma Escalera, A. I., Morones-Ramirez, J. R., Keasling, J. D., & Solis, L. R. (2020). Enhanced production of taxadiene in *Saccharomyces cerevisiae*. *BioRxiv*. Preprint. <https://doi.org/10.1101/2020.06.08.139600>
- Paradise, E. M., Kirby, J., Chan, R., & Keasling, J. D. (2008). Redirection of flux through the FPP branch-point in *Saccharomyces cerevisiae* by down-regulating squalene synthase. *Biotechnology and Bioengineering*, 100(2), 371–378. <https://doi.org/10.1002/bit.21766>
- Peña, A., Álvarez, H., Ramírez, J., Calahorra, M., & Sánchez, N. S. (2015). Effects of high medium pH on growth, metabolism and transport in *Saccharomyces cerevisiae*. *FEMS Yeast Research*, 15(2). <https://doi.org/10.1093/femsyr/fou005>
- Perez-Samper, G., Cerulus, B., Jariani, A., Vermeersch, L., Barraón Simancas, N., Bisschops, M. M. M., & Verstrepen, K. J. (2018). The crabtree effect shapes the *Saccharomyces cerevisiae* lag phase during the switch between different carbon sources. *mBio*, 9(5), e01331–18. <https://doi.org/10.1128/mBio.01331-18>
- Reider Apel, A., Sachs, D., Tong, G. J., d'Espaux, L., Wehrs, M., Garber, M., Nnadi, O., Zhuang, W., Hillson, N. J., Keasling, J. D., & Mukhopadhyay, A. (2016). A Cas9-based toolkit to program gene expression in *Saccharomyces cerevisiae*. *Nucleic Acids Research*, 45(1), 496–508. <https://doi.org/10.1093/nar/gkw1023>
- Sagwan-Barkdoll, L., & Anterola, A. M. (2018). Taxadiene-5 $\alpha$ -ol is a minor product of CYP725A4 when expressed in *Escherichia coli*. *Biotechnology and Applied Biochemistry*, 65(3), 294–305. <https://doi.org/10.1002/bab.1606>
- Valli, M., Sauer, M., Branduardi, P., Borth, N., Porro, D., & Mattanovich, D. (2005). Intracellular pH distribution in *Saccharomyces cerevisiae* cell populations, analyzed by flow cytometry. *Applied and Environmental Microbiology*, 71(3), 1515–1521. <https://doi.org/10.1128/AEM.71.3.1515-1521.2005>
- Walker, K., Ketchum, R. E. B., Hezari, M., Gatfield, D., Goleniowski, M., Barthol, A., & Croteau, R. (1999). Partial purification and characterization of acetyl coenzyme A: Taxa-4(20),11(12)-dien-5 $\alpha$ -ol O-acetyl transferase that catalyzes the first acylation step of taxol biosynthesis. *Archives of Biochemistry and Biophysics*, 364(2), 273–279. <https://doi.org/10.1006/abbi.1999.1125>
- Walker, M. G., & Stewart, G. G. (2016). *Saccharomyces cerevisiae* in the production of fermented beverages. *Beverages*, 2(4), 30. <https://doi.org/10.3390/beverages2040030>
- Wu, J. T., Wu, L. H., & Knight, J. A. (1986). Stability of NADPH: Effect of various factors on the kinetics of degradation. *Clinical Chemistry*, 32(2), 314–319. <http://clinchem.aaccjnl.org/content/32/2/314.abstract>
- Yadav, V. G. (2014). Unraveling the multispecificity and catalytic promiscuity of taxadiene monooxygenase. *Journal of Molecular Catalysis B: Enzymatic*, 110, 154–164. <https://doi.org/10.1016/j.molcatb.2014.10.004>
- Yu, L. X., Amidon, G., Khan, M. A., Hoag, S. W., Polli, J., Raju, G. K., & Woodcock, J. (2014). Understanding pharmaceutical quality by design. *The AAPS Journal*, 16(4), 771–783. <https://doi.org/10.1208/s12248-014-9598-3>
- Zangar, R. C., Davydov, D. R., & Verma, S. (2004). Mechanisms that regulate production of reactive oxygen species by cytochrome P450. *Toxicology and Applied Pharmacology*, 199(3), 316–331. <https://doi.org/10.1016/j.taap.2004.01.018>
- Zhou, K., Qiao, K., Edgar, S., & Stephanopoulos, G. (2015). Distributing a metabolic pathway among a microbial consortium enhances production of natural products. *Nature Biotechnology*, 33(4), 377–383. <https://doi.org/10.1038/nbt.3095>

## SUPPORTING INFORMATION

Additional supporting information may be found online in the Supporting Information section.

**How to cite this article:** Walls LE, Malcı K, Nowrouzi B, et al. Optimizing the biosynthesis of oxygenated and acetylated Taxol precursors in *Saccharomyces cerevisiae* using advanced bioprocessing strategies. *Biotechnology and Bioengineering*. 2021;118:279–293. <https://doi.org/10.1002/bit.27569>